Mechanisms of Class I Restricted Immunopathology. A Transgenic Mouse Model of Fulminant Hepatitis

By Kazuki Ando,* Takashi Moriyama,* Luca G. Guidotti,* Susanne Wirth,* Robert D. Schreiber,‡ Hans Jürgen Schlicht,§ Shao-nan Huang,* and Francis V. Chisari*

*From the *Department of Molecular and Experimental Medicine, The Scripps Research Institute, La Jolla, California 92037; the ‡Department of Pathology, Washington University School of Medicine, St. Louis, Missouri 63110; and the §Department of Virology, Institute of Microbiology, University of Ulm, Oberer Eselsberg, D-7900, Ulm, Germany*

Summary

The molecular and cellular mechanisms responsible for cytotoxic T lymphocyte (CTL)–induced immunopathology are not well defined. Using a model in which hepatitis B surface antigen (HBsAg)–specific CTL cause an acute necroinflammatory liver disease in HBsAg transgenic mice, we demonstrate that class I–restricted disease pathogenesis is an orderly, multistep process that involves direct as well as indirect consequences of CTL activation. It begins (step 1) almost immediately as a direct antigen-specific CTL-target cell interaction that triggers the HBsAg-positive hepatocyte to undergo programmed cell death (apoptosis). It progresses (step 2) within hours to a focal inflammatory response in which antigen-nonspecific lymphocytes and neutrophils amplify the local cytopathic effect of the CTL. The most destructive pathogenetic function of the CTL, however, is to secrete interferon γ when they encounter antigen in vivo, thereby activating the intrahepatic macrophage and inducing a delayed-type hypersensitivity response (step 3) that destroys the liver and kills the mouse. We propose that the principles illustrated in this study are generally applicable to other models of class I–restricted, CTL-induced immunopathology, and we suggest that they contribute to the immunopathogenesis of viral hepatitis during hepatitis B virus infection in humans.

Viral clearance and disease pathogenesis in noncytopathic viral infections are generally thought to represent linked consequences of an MHC class I–restricted CTL response to viral antigens expressed by infected cells. Since class I–restricted CTL are defined by their ability to specifically recognize and destroy target cells in vitro, it is generally assumed that this is also their principal function in vivo. This has never been proven, however. In fact, with respect to viral clearance, recent studies have demonstrated that HIV-specific CTL can control HIV replication by a noncytolytic mechanism (1, 2), and HSV replication can be prevented by HSV-specific CTL at noncytolytic E/T cell ratios in vitro (3). Furthermore, influenza virus–specific CTL can lead to strain-specific viral clearance in vivo, without any attendant pathological consequences (4), and lymphocytic choriomeningitis virus (LCMV)[1] can be cleared from the spleen, by the adoptive transfer of as few as 200 LCMV-specific CTL (5). Thus, it would appear that the virus control function of class I–restricted CTL can be expressed independently of their cytotoxic potential in vitro and in vivo.

With respect to tissue injury, although class I–restricted, antigen-specific CTL can cause allograft rejection (6, 7), tumor regression (8, 9), or necroinflammatory diseases in infected mice (10, 11), direct lysis of target cells by the CTL has not been demonstrated in these models. Instead, it has been suggested that CTL-induced indirect secondary events might play a dominant role in class I–restricted tissue injury (12, 13), like the delayed-type hypersensitivity (DTH) reaction plays in class II–restricted autoimmune disease models, such as experimental autoimmune encephalitis (14–16), thyroiditis (17), orchitis (18), and insulin-dependent diabetes in the nonobese diabetic mouse (19).

We have previously demonstrated that class I–restricted hepatitis B surface antigen (HBsAg)–specific spleen cells and cloned CTL cause a necroinflammatory disease when they are injected into HBsAg transgenic mice (20). Recently, we have demonstrated that such CTL directly bind and induce the cytological changes characteristic of programmed cell death (apoptosis) in HBsAg-positive hepatocytes shortly after in-

[1] *Abbreviations used in this paper:* BrdU, bromodeoxyuridine; DTH, delayed type hypersensitivity; ER, endoplasmic reticulum; HBV, hepatitis B virus; HBsAg, hepatitis B surface antigen; LCMV, lymphocyte choriomeningitis virus; LDH, lactic dehydrogenase; sALT, serum alanine aminotransferase.

jection into such animals (Ando, K., T. Moriyama, S. Wirth, L. G. Guidotti, R. D. Schreiber, H. J. Schlist, S.-n. Huang, and F. V. Chisari, manuscript submitted for publication). In the current study we show that that disease severity is not primarily determined by the direct cytotoxic potential of the CTL in this model. Instead, it depends on CTL-activated downstream events involving the recruitment of antigen-nonspecific inflammatory cells, as well as amplification mechanisms that the CTL activate by releasing IFN-γ when they recognize antigen in vivo, and that the intrinsic sensitivity of the target hepatocyte to destruction by these mechanisms contributes significantly to the severity of the resultant disease. Furthermore, it is apparent that class I–restricted disease pathogenesis, in this model, is an orderly, multistep process that progresses from direct CTL-induced single cell necrosis to a focal inflammatory response that locally amplifies the cytopathic effect of the CTL, and that it culminates in a generalized DTH reaction that can destroy the liver and kill the mouse.

Materials and Methods

HBsAg-specific CTL. Two independently derived $CD3^+$, $CD4^-$, $CD8^+$ CTL clones (designated 6C2 and D10) that have been described in detail elsewhere (20, Ando, K. et al., manuscript submitted for publication) were used in this study. Both clones are Ld restricted, recognize an epitope (IPQSLDSWWTSL) that is located between residues 28–39 of HBsAg, and secrete IFN-γ but not (TNF-α) after antigen stimulation in vitro (Ando, K. et al., manuscript submitted for publication). They were maintained by weekly restimulation with irradiated P815 cells that stably express the hepatitis B virus (HBV) large envelope protein (ayw subtype) containing HBsAg, as previously described (20, and Ando, K. et al., manuscript submitted for publication).

HBV Transgenic Mice. Production and characterization of the transgenic mouse lineages used in these studies have been previously described (21–25). These lineages were selected because they do not develop any evidence of spontaneous liver disease and because they display lineage-specific differences in hepatocellular HBsAg expression that permit investigation of several quantitative and qualitative aspects of class I–restricted CTL-target cell interaction in vivo.

Most studies were performed in lineage 107-5D (official designation Tg[Alb-1,HBV]Bri66), (inbred B10.D2, H-2^d) in which, constitutively, the HBV envelope coding region is under the control of the mouse albumin promoter. The HBV large envelope polypeptide forms long nonsecretable filamentous HBsAg particles that are retained within the endoplasmic reticulum (ER) of the hepatocyte where they are readily detectable immunohistochemically (21, and see Fig. 4 *D*, this paper). Selected experiments were also performed with mice in which this transgene had been backcrossed onto a B10.S (H-2^s) background (lineage 107-5S).

Lineage 23-3 (official designation Tg[MT-1,HBV]Bri28), (inbred C57Bl/6, H-2^b), expresses the HBV large envelope polypeptide under the control of the zinc inducible mouse metallothionein promoter. In the absence of dietary zinc supplementation, an internal HBV promoter, which is present within the envelope coding region in the transgene, drives expression of the HBV major envelope polypeptide which is effectively secreted by the hepatocyte into the circulation such that hepatocellular HBsAg is barely detectable immunohistochemically (21, and see Fig. 3 *A*, this paper). Activation of the metallothionein promoter by oral zinc administration leads to production of the HBV large envelope polypeptide by the hepatocyte, resulting in retention of HBsAg in the ER (as in lineage 107-5 above), where it is detectable principally in periportal hepatocytes close to the point of entry of the circulation into the hepatic lobule (21, and see Fig. 3 *C*, this paper).

Lineage pFC80-219 (official designation Tg[HBs,HVB]Chi219), (inbred C57Bl/6, H-2^b) expresses only the HBV major envelope polypeptide under the transcriptional control of HBV regulatory elements. These mice secrete large quantities of HBsAg into the circulation and do not retain any immunohistochemically detectable HBsAg in their hepatocytes (23, 24, and see Fig. 4 *F*, this paper). For these studies, lineages 23-3 and pFC80-219 were backcrossed one generation against B10.D2 to produce H-2^{bxd} F_1 hybrids before injection of the H-2^d-restricted CTL (23-3^{bxd} and pFC80-219^{bxd}).

The intrahepatic distribution of HBV antigens was assessed by the indirect immunoperoxidase method using 3-amino-9-ethyl carbazole (Shandon-Lipshaw, Pittsburgh, PA) as a coloring substrate, as previously described (25). Duplicate sections were also stained with normal rabbit serum as the primary antibody to serve as negative controls. HBsAg positive human and transgenic mouse liver tissue served as assay controls.

Disease Model. 5 d after the last stimulation, CTL were washed, counted, suspended in HBSS containing 2% FCS, and injected intravenously or intraperitoneally into transgenic and nontransgenic recipients. Hepatocellular injury was monitored biochemically by measuring serum alanine aminotransferase (sALT) activity (25). Results were expressed as mean sALT activity ± SEM and differences between experimental and control groups were assessed for statistical significance by Student's *t* test. Mice were killed by cervical dislocation, and necropsy was performed. Tissue samples were fixed in 10% zinc buffered formalin (Anatek, Ltd, Battle Creek, MI), embedded in paraffin, sectioned (3 μ) and stained with hematoxylin and eosin as described (25). The number of hepatocytes and intrahepatic inflammatory cells were counted in at least 50 high power (×400) fields and the results were expressed as the number of cells per mm^2 of liver tissue. Standard cytopathological criteria were used to define the various components of the inflammatory response. Lymphocytes and macrophages were identified immunohistochemically in snap-frozen, acetone-fixed tissue using rat mAbs to L3T4, Lyt-2, and Mac-1 according to the manufacturer's instructions (Boehringer Mannheim Corp., Indianapolis, IN).

Quantitation of Intrahepatic CTL. In selected experiments, CTL clones were incubated with 50 mM bromodeoxyuridine (BrdU; Sigma Chemical Co., St. Louis, MO) for 2 d in vitro before injection into HBV transgenic mice. Immunocytochemical analysis before injection (see below) revealed that >98% of the CTL were labeled by this procedure, and functional analysis revealed that the cytolytic activity of the CTL was unaffected by the BrdU labeling process. To detect BrdU-positive CTL in tissue, paraffin-embedded tissue sections were treated with 3% H_2O_2 at room temperature and with 0.05% pepsin in 0.01N HCl (37°C, 20 min). Slides were rinsed and incubated in 1 N HCl (60 min, room temperature), washed with PBS (pH 7.4), blocked with normal goat serum for 30 min at room temperature, and incubated overnight at 4°C in a humid chamber with a 1/100 dilution of mouse monoclonal anti-BrdU antibody (Becton Dickinson & Co., Mountain View, CA). After washing with PBS, the tissue sections were incubated with biotinylated goat $F(ab')_2$ anti–mouse IgG (Sigma Chemical Co.) at a 1/50 dilution (30 min, 37°C). The slides were then washed with PBS and incubated with Streptavidin–horseradish peroxidase conjugate (Extravidin; Sigma Chemical Co.) at a 1/600 dilution

(30 min, 37°C). A dark brown reaction product was produced with Diaminobenzidine (DAB)-Cobalt-H_2O_2 (5 min, room temperature), and the slides were counterstained with hematoxylin and eosin before mounting.

Functional Role of Host-derived Inflammatory Cells. Groups of mice received 900 rad of gamma irradiation (Gamma Cell 40; Atomic Energy of Canada, Ont., Canada) 6 d before the transfer of CTL, thereby reducing the number of spleen cells more than 100-fold before CTL injection (data not shown). Other mice were injected intraperitoneally with 1 ml of carrageenan (type 2; Sigma Chemical Co.) dissolved and sterilized by boiling in sterile nonpyrogenic PBS, at a concentration of 2 mg/ml as previously described (26, 27) on days −4, −3, −2, −1, and 0 relative to CTL administration. Control mice received 1 ml of PBS at the same times before CTL administration. Selected animals were injected intravenously with India ink (0.2 ml; CII/1431a, diluted threefold; Pelikan Spezialtusche, Hannover, Germany) 24 h before killing (28) to assess the influence of irradiation or carrageenan injection on tissue macrophages.

Role of IFN-γ and TNF-α. To evaluate the role of IFN-γ and TNF-α in the disease process, CTL were administered 24 h before or after the intraperitoneal injection of hamster mAbs H22 and TN3 19.12 specific for murine IFN-γ and TNF-α, respectively (29, 30). Purified hamster IgG (Jackson ImmunoResearch, West Grove, PA) was used as a control antibody. All antibodies were diluted to a concentration of 250 mg/200 ml with nonpyrogenic PBS (GIBCO BRL, Gaithersburg, MD) just before administration.

Mouse Hepatocyte Culture. To assess the direct hepatocytotoxic potential of IFN-γ and TNF-α, primary transgenic and nontransgenic hepatocytes were incubated with various concentrations of recombinant murine IFN-γ (sp act 5.2×10^6 U/mg) and recombinant murine TNF-α (sp act 1.2×10^6 U/mg), which were generously provided by Dr. Susan Kramer (Genentech, Inc., South San Francisco, CA). For these studies, hepatocyte suspensions were prepared by perfusion of transgenic and nontransgenic mouse livers with 20 ml of Ca^{2+} free PBS containing EGTA (190 mg/liter; Sigma Chemical Co.) and 30 ml of HBSS containing collagenase (500 mg/liter, 0.9 U/mg; Serva, Westbury, NY) and $CaCl_2$ (420 mg/liter; Sigma Chemical Co.) at 37°C. The cells were suspended in EHAA medium (GIBCO BRL) containing 10% FCS at 4°C, filtered through No. 150 mesh, and centrifuged three times (50 *g*, 1 min). Purified hepatocytes were resuspended (5×10^5/ml) in the same medium and plated (2 ml/well) in 6-well plates (Corning Inc., Corning, NY). 4 h later, the supernatant was removed from the adherent cells and replaced with 2 ml fresh EHAA medium containing 10% FCS, epidermal growth factor (20 ng/ml) and insulin (10^{-9} M; all from Sigma Chemical Co.). After overnight incubation, the cells were fed with 1 ml of fresh media. 24 h later, the supernatants and cell lysates (1% Triton X, 1 ml/well) were analyzed for ALT or lactic dehydrogenase (LDH) activity as previously described (25). Cytokine-mediated cytotoxic activity was expressed as percent ALT or LDH release calculated as follows 100 × (ALT or LDH in medium/ALT or LDH in Triton X).

Results

HBsAg-specific CTL Induce an Acutely Fatal Necroinflammatory Liver Disease (Fulminant Hepatitis) in HBsAg Transgenic Mice. Two independently derived $CD3^+$, $CD4^-$, $CD8^+$ CTL clones, designated 6C2 and D10 were used in this study because of their excellent cytotoxic and growth characteristics in vitro. Both clones, studied sequentially over a 2-yr period, displayed virtually identical behavior in vitro and in vivo. Most studies were performed by injection of clone 6C2 into lineage 107-5D, with confirmatory studies performed in other lineages and with clone D10. Upon injection into HBsAg-positive transgenic mice lineage (107-5D), both clones D10 and 6C2 were shown to induce an acute, H-2^d restricted, lethal necroinflammatory liver disease that reaches peak severity within 24–72 h and resolves completely (in survivors) 7–10 d later.

Sex Dependence. As shown for clone 6C2 (Fig. 1 *A*), the severity of liver disease (measured biochemically as sALT activity) was approximately four times greater in males (13,650 ± 2,130 U/liter) than in females (3,740 ± 1,267 U/liter) ($p < 0.005$) after i.v. administration of 10^7 CTL (Fig. 2 *A*). The same is true for the disease severity observed after CTL administration to lineages 23-3 and pFC80-219 (data not shown). The reason for this difference has not been defined, but it might be due to higher intracellular concentrations of HBsAg in males than in females. Indeed, we have shown (25) that intrahepatic HBsAg content is greater in males than in females in an independent lineage (50-4) that contains the same transgene as lineage 107-5. Because of this difference, all subsequent studies were performed in males.

Route of Administration. Disease severity was also influenced by the route of CTL administration (Fig. 1 *B*). sALT levels rose more than 100-fold after the intravenous injection of 10^7 CTL into lineage 107-5D males, as compared with only a 10-fold increase after intraperitoneal injection. Using BrdU-labeled CTL, the number of CTL that localized to the liver after intraperitoneal injection was found to be less than that observed after intravenous injection (data not shown).

CTL Dose and MHC Dependence. Disease severity was also strictly CTL dose dependent in lineage 107-5D recipients in which the transgene was expressed in the context of an H-2^d genetic background (Fig. 2 *A*). Liver disease was detectable biochemically as progressively increasing sALT activity at CTL doses above 10^5 CTL per mouse. At 10^7 CTL per mouse, the resultant liver disease was severe enough to be fatal within 96 h in 7/15 recipients (46.7%), and it was fatal for all 10 mice (100%) that received 1.5×10^7 CTL (Fig. 2 *B*). In the same study, 10^7 CTL failed to induce liver disease in transgenic recipients that expressed the same transgene in the context of an H-2^s genetic background (Fig. 2 *A*), in keeping with the demonstration that the CTL are L^d restricted in vitro (Ando, K. et al., manuscript submitted for publication). Importantly, as shown in Fig. 2, treatment of the mice with antibodies to IFN-γ before CTL administration completely protected the mice against fatal liver disease (see below for additional details).

Intrahepatic HBsAg Content. Using lineage 23-3 H-2^{bxd} F_1 males derived from transgenic (H-2^b) parents that had been bred with nontransgenic B10.D2 (H-2^d) mates, we demonstrated that the severity of liver disease was directly related to the total intrahepatic HBsAg content in the recipients. Under baseline conditions in this lineage, the hepatocytes secrete HBsAg so rapidly that it is not detectable in the liver (Fig. 3 *A*) even though it can reach 10-fold higher

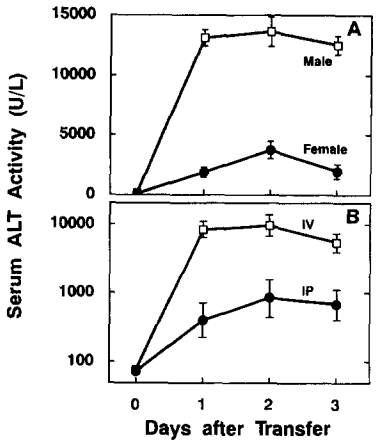

Figure 1. CTL-induced liver disease in HBsAg-positive transgenic mice depends on the route of administration and the sex of the recipient. (*A*) CTL-induced liver disease in lineage 107-5D recipients is more severe in males than in females. Serum ALT activity was analyzed at varying times relative to the injection of 10^7 CTL (clone 6C2) into groups of three age-matched male and female littermates. (*B*) 10^7 CTL (clone 6C2) were injected either intravenously or intraperitoneally into lineage 107-5D transgenic male recipients.

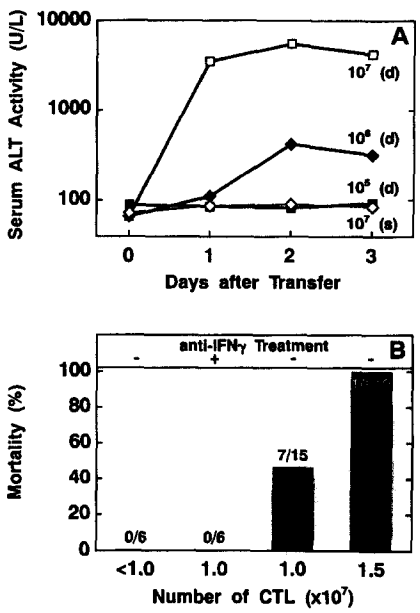

Figure 2. CTL-induced liver disease and mortality depends on the number of CTL administered and the MHC class I haplotype of the recipient. (*A*) sALT activity was monitored daily after the injection of varying doses of clone 6C2 CTL into lineage 107-5D (H-2^d) and 107-5S (H-2^s) transgenic mice. (*B*) Results reflect mortality after intravenous injection of 10^5, 10^6, 10^7, or 1.5 × 10^7 CTL into groups of 6, 6, 15, and 10 lineage 107-5D male recipients, respectively. Six animals were injected with 10^7 CTL 24 h after the intraperitoneal administration of 500 μg of hamster anti-IFN-γ mAb.

concentrations in the blood than lineage 107-5 (21). In contrast, when synthesis of the HBV large envelope polypeptide is induced by activating the metallothionein promoter with oral zinc sulfate, nonsecretable filamentous HBsAg particles are formed and retained within the ER where they can be detected immunohistochemically as cytoplasmic HBsAg (Fig.

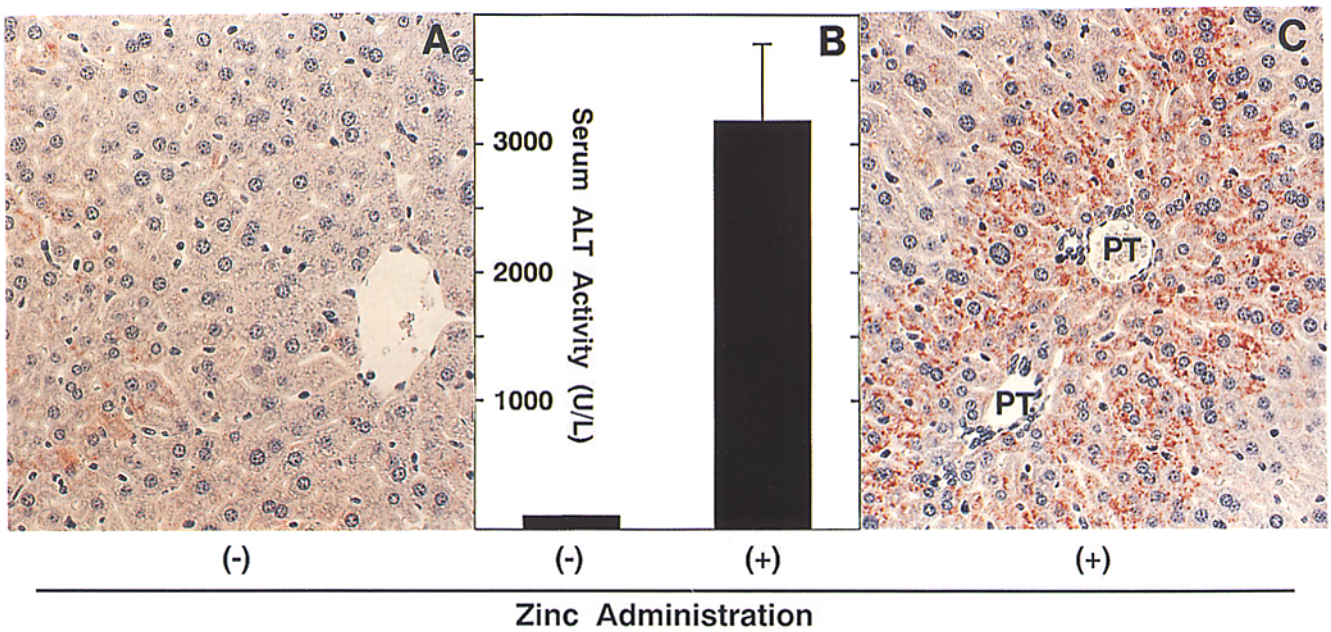

Figure 3. The severity of CTL-induced liver disease is a function of HBsAg retention by the hepatocyte. Lineage 23-2^{bxd} transgenic males containing the zinc inducible mouse metallothionein promoter were injected with 10^7 CTL (clone 6C2). Selected animals were pretreated with zinc sulfate as a 0.75% solution in the drinking water for 14 d before CTL administration. (*A* and *C*) The intrahepatic content of HBsAg before and after zinc administration (immunocytochemical staining for HBsAg, ×200). Note the presence of very rare, faintly HBsAg-positive hepatocytes (*red stain*, *A*), and the abundance of moderately strongly positive hepatocytes in the periportal area (*PT*, portal tract, *C*) of the hepatic lobule. (*B*) The sALT activity on day 2 after CTL administration to zinc treated (+) and untreated (−) mice. Experiments were performed in triplicate.

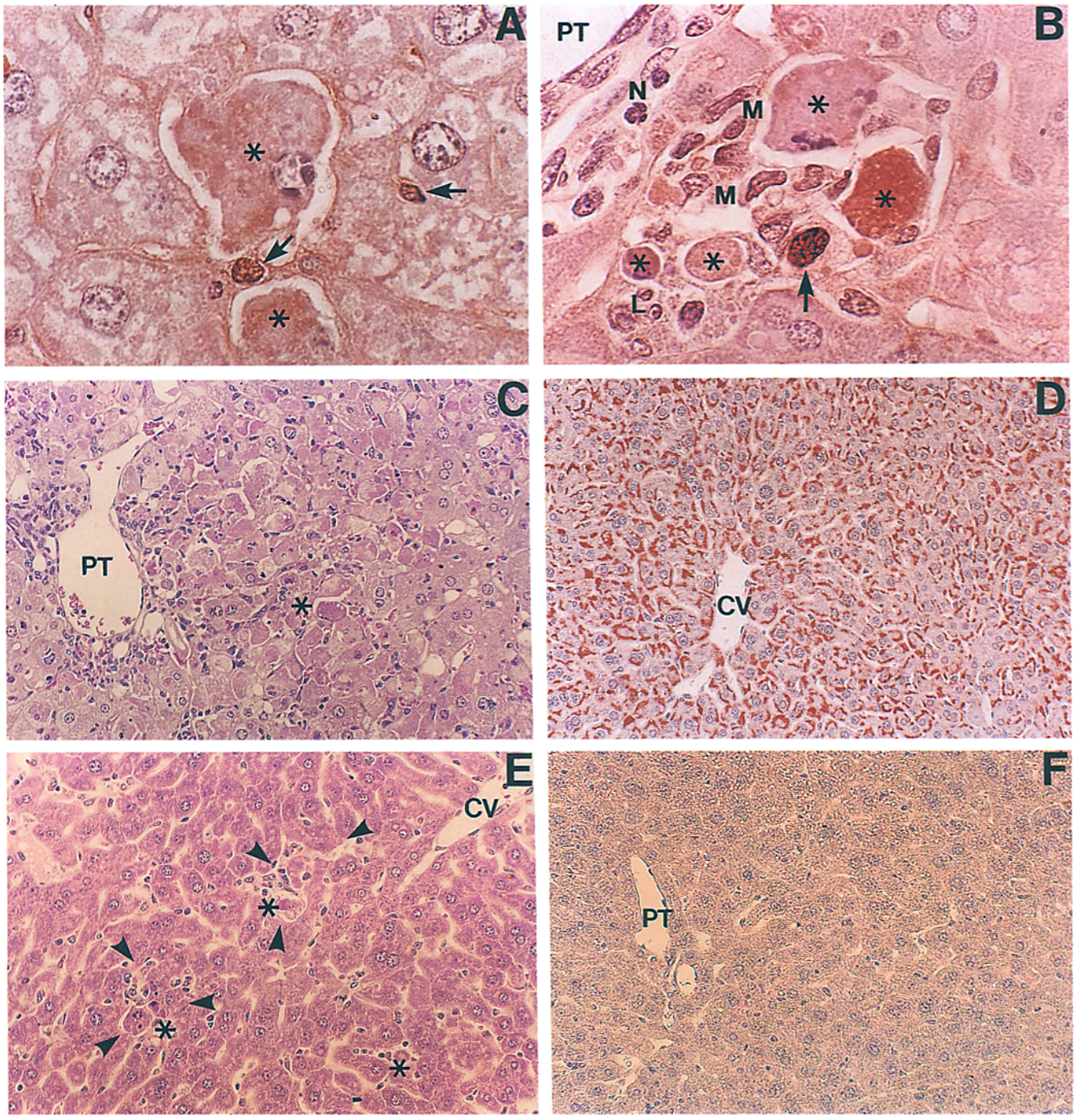

Figure 4. Sequential histopathological manifestations of fulminant hepatitis after CTL administration in transgenic mice. Histopathological characteristics of transgenic mouse livers observed 1–4 h (*A*, BrdU stain, original magnification ×960), 4–12 h (*B*, BrdU stain, ×960), and 72 h (*C*, hematoxylin and eosin, ×200) after CTL administration to transgenic mice from lineages 107-5D and pFC80-219D (*E*, hematoxylin and eosin, ×200) the baseline intrahepatic HBsAg content of which is demonstrated by immunohistochemical staining for HBsAg in *D* (107–5D, ×200) and *F* (pFC80-219D, ×200). (*Asterisks*) Apoptotic hepatocytes; (*arrows*) BrdU-positive CTL; (*arrowheads*) necroinflammatory foci; (*PT*) portal tract; (*CV*) central vein. See text for description.

3 *C*), similar to lineage 107-5 (Fig. 4 *D*) in which the large envelope polypeptide is constitutively expressed under the control of the albumin promoter (21). Interestingly, the CTL caused little or no hepatocellular injury in lineage 23-3^{bxd} unless HBsAg was retained by the hepatocyte (Fig. 3 *B*), suggesting that the severity of CTL-induced liver disease is determined by the number of hepatocytes that retain HBsAg or by the concentration of HBsAg within each cell, or both.

Histopathological and Quantitative Morphometric Analysis of the Intrahepatic Inflammatory Cell Infiltrate in the Context of HBsAg Retention (Lineage 107-5) or Secretion (Lineage pFC80-219^{bxd}) by the Hepatocyte. Histopathological (Fig. 4) and quantitative morphometric (Fig. 5) analysis of hematoxylin and eosin stained tissue sections was performed at frequent intervals throughout the course of the disease after the injection of 10^7 CTL into male 107-5D recipients. Lineage pFC80-219^{bxd} males were also examined histologically at a single time point (48 h) after CTL injection. In selected instances, the CTL were labeled with BrdU before injection to permit them to be identified immunohistochemically in the tissue.

The disease appeared to progress through three distinct histopathological stages in lineage 107-5D. The first stage (step 1) was heralded by the entry of BrdU-labeled CTL into the hepatic parenchyma, within 1 h of intravenous CTL administration as shown in Figs. 4 *A* (arrow) and 5 *B*. Over the next 4 h, CTL were observed to be attached to hepatocytes that displayed the diagnostic cytological feature of apoptosis (Ando, K. et al., manuscript submitted for publication). Specifically, the CTL-associated hepatocytes displayed margination of nuclear chromatin and cytoplasmic condensation and fragmentation together with cellular shrinkage (Fig. 4 *A*, asterisk), producing the well-known acidophil, or Councilman, bodies that represent cytoplasmic fragments of apoptotic hepatocytes (Ando, K. et al., manuscript submitted for publication) and are characteristic of viral hepatitis (31, 32). No other inflammatory cells were detectable in the vicinity of these lesions, or elsewhere within the liver at this time, indicating that the CTL were solely responsible for this effect. The sALT levels were normal or only very slightly elevated during this interval (Fig. 5 *A*), suggesting either that this enzyme was not released during this process, or that the number of apoptotic hepatocytes was insufficient to yield a significant increase in sALT activity.

With the passage of time, the number of BrdU-positive CTL in the liver increased, reaching a plateau of approximately 22 CTL per mm^2 of liver tissue 4–12 h after injection (Fig. 5 *B*). During this interval, the number of BrdU-positive CTL (Fig. 4 *B*, arrow)–associated apoptotic hepatocytes (Fig. 4 *B*, asterisks) also increased progressively, and many necroinflammatory foci appeared, indicating onset of the second stage (step 2) in the disease process. In these foci, the CTL were surrounded by unlabeled (therefore host derived) inflammatory cells, including cytologically distinguishable neutrophils, lymphocytes, and macrophages (Fig. 4 *B*, N, M, and L), and necrotic hepatocytes were observed to be spatially distant from the labeled CTL, suggesting that they might have been destroyed by non-CTL constituents within the necroinflammatory foci. Concomitant with the development of necroinflammatory foci 4–12 h after CTL injection, the number of cytologically apparent dead and degenerating hepatocytes in the liver increased substantially, and the sALT activity levels began to rise (Fig. 5 *A*).

24–72 h after CTL injection, hepatocellular necrosis became widespread throughout the lobule (panlobular), marking the third stage (step 3) of the disease. During this period,

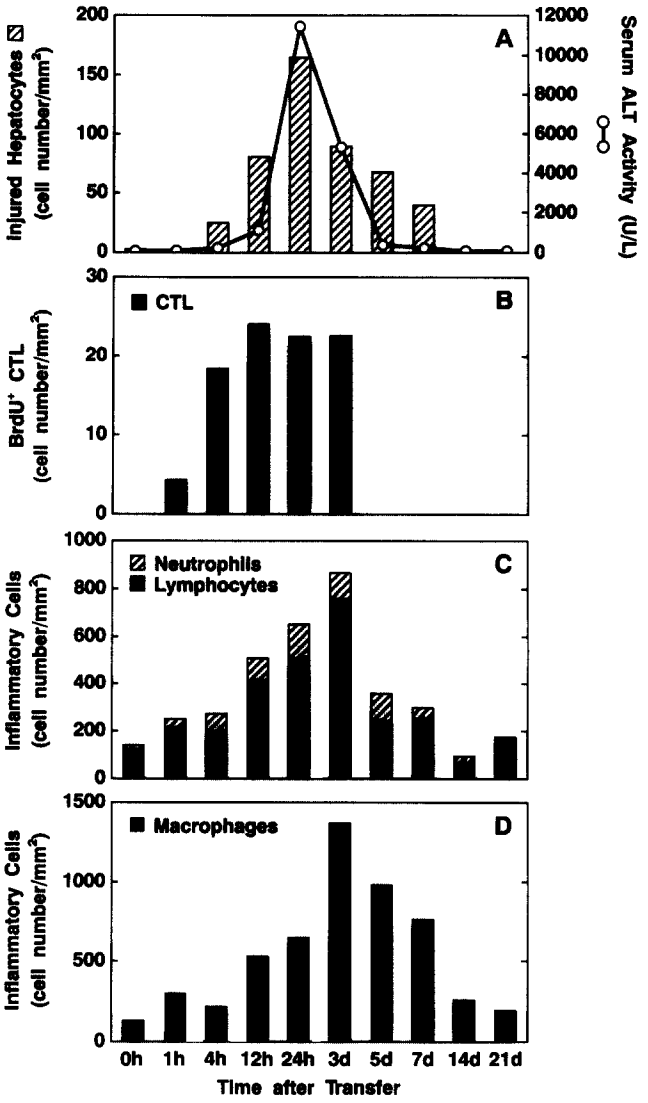

Figure 5. Kinetics and cell type of intrahepatic inflammatory infiltrate and liver cell injury. Quantitative morphometry of injured hepatocytes and intrahepatic inflammatory cells at multiple time points after the injection of 10^7 clone 6C2 CTL into lineage 107-5 male transgenic mice. A minimum of 50 high power (×400) fields representing 2 mm^2 of liver tissue were examined. The number of dead and degenerating hepatocytes (*A*), BrdU-positive CTL (*B*), neutrophils and lymphocytes (*C*), and tissue macrophages (*D*) present in 3-μM-thick sections were expressed as the number of cells per mm^2 of liver tissue. The results reflect the mean of two observations (two mice) for each point. Serum ALT activity was measured at the times indicated.

the number of necrotic and degenerating hepatocytes and the sALT levels reached a peak (Fig. 5 *A*) from which they subsequently declined in the surviving animals. Histopathologically, at these time points, the vast majority of hepatocytes were either frankly necrotic or displayed prelytic changes such as extreme cytoplasmic hydropic degeneration and ballooning, or apoptosis, in the context of an overwhelming inflammatory reaction (Fig. 4 *C*). Coincidentally, the number of BrdU-negative, host-derived inflammatory cells also increased but, unlike the BrdU-positive CTL which reached a plateau by 12 h after CTL injection (Fig. 5 *B*), they continued to rise

for 72 h (Fig. 5, *C* and *D*), eventually outnumbering the CTL by at least 100-fold before they started to decline. Frozen sections from selected livers were examined immunohistochemically for lymphocyte and macrophage markers at this time point. Although precise quantitation was not possible, it was clear that cells of the monocyte/macrophage lineage dominated the inflammatory infiltrate, and that a less abundant mixed population of L3T4 and Lyt-2-positive lymphocytes was also present, confirming the cytomorphological observations described above.

The foregoing disease occurred in the context of hepatocellular HBsAg retention in lineage 107-5D (Fig. 4 *D*). To investigate the possibility that retention of HBsAg might contribute to the severity of liver disease in this model, as it does after the injection of bacterial LPS and IFN-γ into the same lineage of mice (24), we examined the histopathological characteristics of the CTL-induced liver disease in lineage pFC80-219D whose hepatocytes do not retain immunohistochemically detectable HBsAg (Fig. 4 *F*). Interestingly, peak sALT levels achieved after CTL injection were <5% as high (288 ± 47.9 U/liter, $n = 5$) as the levels routinely achieved in lineage 107-5D. Histopathologically, these animals displayed widely scattered apoptotic hepatocytes associated with BrdU-positive CTL (step 1) during the first few hours after CTL injection, and at the peak of disease, the liver contained multiple, small necroinflammatory foci (Fig. 4 *E*, arrowheads) containing apoptotic hepatocytes (Fig. 4 *E*, asterisks) that resembled a mild form of step 2 seen in lineage 107-5D (Fig. 4 *B*). Importantly, the liver disease appeared to stop at this stage in lineage pFC80-219D. The data suggest, therefore, that HBsAg retention appears to play a very important, perhaps critical role in disease progression from step 2 to step 3 in this model, presumably by sensitizing the hepatocyte to additional events (see below) that lead to widespread panlobular necrosis and hepatic failure.

The Role of IFN-γ. Since clones D10 and 6C2 produce IFN-γ in vitro upon antigenic stimulation (Ando, K. et al., manuscript submitted for publication), and since we have previously shown that the HBsAg-positive hepatocyte is exquisitely susceptible to destruction by an IFN-γ–dependent pathway in vivo (24), we examined the ability of monoclonal anti-IFN-γ antibodies to mitigate the induction of liver disease by the CTL. As shown in Fig. 6 *A* for clone 6C2, the prior administration of anti-IFN-γ resulted in virtually complete inhibition (97% reduction) of CTL-induced liver cell injury (peak sALT activity 590 ± 170 U/liter compared with 17,883 ± 1,011 U/liter) in the control group ($p < 0.000005$). Importantly, none of the six anti-IFN-γ–treated mice died after CTL injection, whereas the same number of CTL have been shown to be lethal for 7/15 age- and sex-matched animals that had not been pretreated with these antibodies (Fig. 2). Furthermore, when the anti-IFN-γ antibodies were administered 24 h after the CTL, when sALT activity was >7,000 U/liter, the course of the disease was promptly reversed and disease resolution was noticeably accelerated, such that sALT levels in the anti-IFN-γ–treated mice were significantly lower ($p < 0.05$) than the hamster IgG–treated control mice at all time points examined (data not shown).

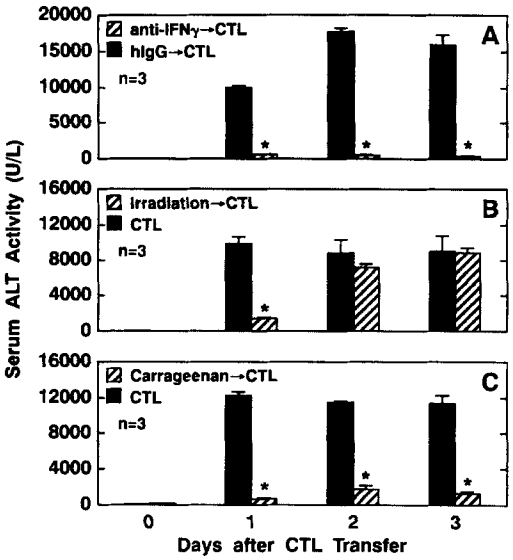

Figure 6. CTL-induced liver disease is mediated principally by IFN-γ. Groups of three lineage 107-5D males were either injected intraperitoneally with 500 μg of hamster mAb to IFN-γ or hamster IgG (*A*), or they were irradiated (900 rad) (*B*), or injected intraperitoneally with carrageenan (*C*) 1 d, 6 d, or daily for 5 d, respectively, before the injection of 10^7 CTL. The severity of the resultant liver disease was measured as sALT activity. All points marked (*) are statistically significantly lower than the corresponding group of three age- and sex-matched mice simultaneously injected with the same number of 6C2 CTL.

The only histological abnormalities observed in lineage 107-5D mice that had been pretreated with antibodies to IFN-γ was the presence of a few small necroinflammatory foci (Fig. 7 *B*, arrowheads) containing apoptotic hepatocytes (Fig. 7 *B*, asterisks), similar to the early focal lesions normally observed in the absence of anti-IFN-γ treatment in this lineage (Fig. 4 *B*) and like the focal lesions characteristic of the most advanced stage of disease seen in lineage pFC80-219D (Fig. 4 *E*). Importantly, there was no evidence of the widespread hepatocellular necrosis seen in control mice after CTL injection (Figs. 4 *C* and 7 *A*) even though the number of BrdU-labeled CTL present in the liver was the same as in control mice not injected with the anti-IFN-γ antibodies (data not shown). This correlated with a prominent reduction in sinusoidal lining cell hyperplasia together with a substantial decrease in the other components of the host-derived inflammatory response (compare Fig. 7, *A* and *B*). These findings suggest that IFN-γ triggers the widespread hepatocellular necrosis characteristic of step 3 of the disease process, but that it appears not to be involved in the induction of hepatocellular apoptosis or the development of necroinflammatory foci.

In contrast to these results, mAbs to TNF-α were only modestly protective against the CTL-induced liver disease. Pretreatment of CTL recipients with anti-TNF-α reduced sALT levels by ~30% ($p < 0.05$, not shown) suggesting that TNF-α plays a much less important role than IFN-γ, consistent with the observation that CTL clone 6C2 does not secrete TNF-α in sufficient amounts to be detected in bioassays in vitro (Ando, K. et al., manuscript submitted for publication). To determine if either of these cytokines are directly

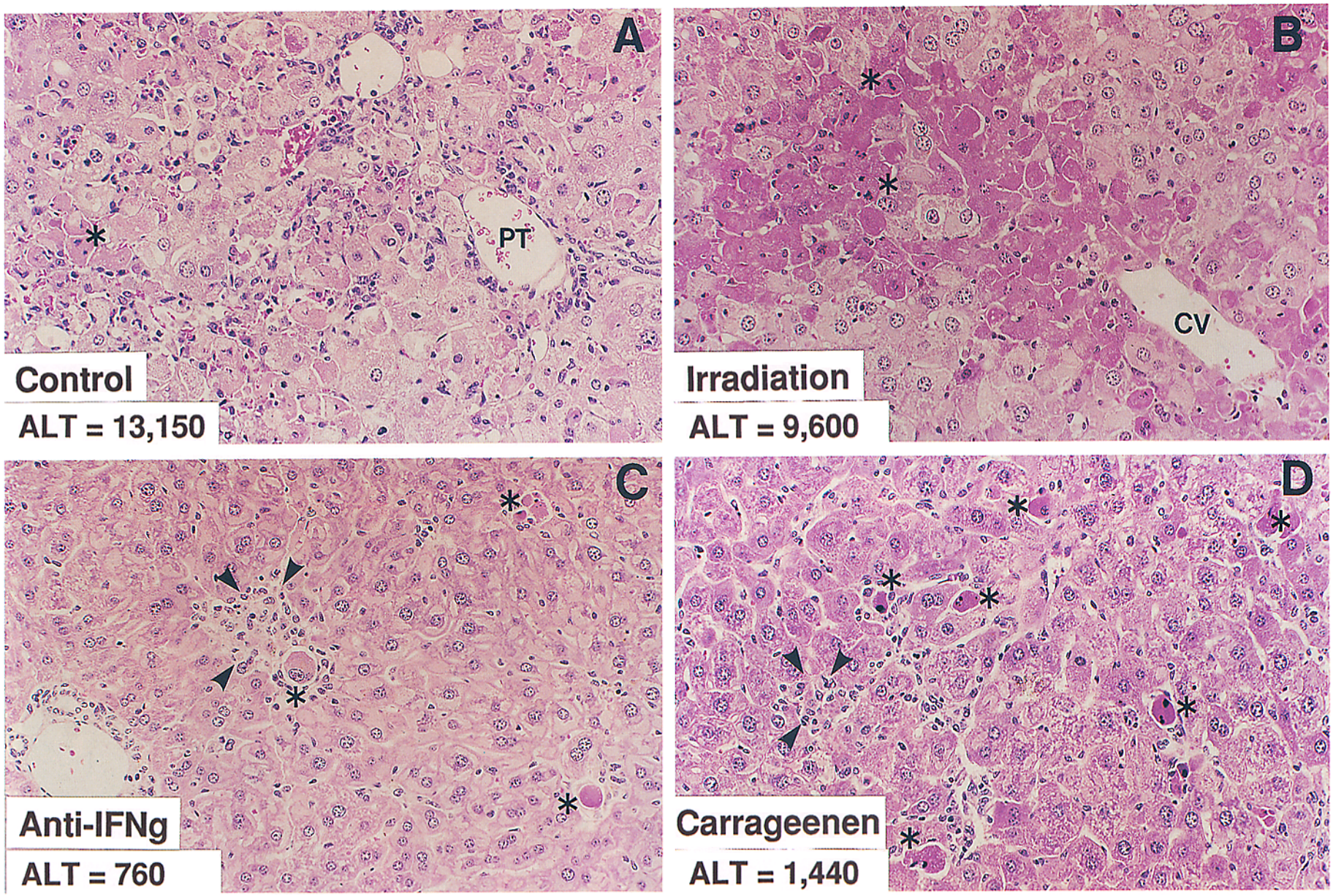
A
PT
Control
ALT = 13,150
B
CV
Irradiation
ALT = 9,600
C
Anti-IFNg
ALT = 760
D
Carrageenen
ALT = 1,440

cytotoxic for the HBsAg-positive hepatocyte, we monitored the release of ALT and LDH from primary cultures of lineage 107-5D hepatocytes after 24 h of in vitro incubation with up to 25,000 U/liter of recombinant IFN-γ or 5,000 U/liter of recombinant TNFα. Neither cytokine was hepatocytotoxic to primary transgenic or nontransgenic hepatocytes in vitro (data not shown), suggesting that the cytopathic effect of these cytokines, especially IFN-γ, in vivo is indirect, presumably by recruitment and activation of antigen nonspecific host inflammatory cells. In separate studies, we also showed that the cytolytic activity of clones D10 and 6C2 are not mediated by IFN-γ in vitro (not shown).

Effect of Irradiation. To examine the role of host inflammatory cells in the pathogenesis of CTL-induced liver disease, mice were irradiated (900 rad) 6 d before CTL administration in order to destroy the radiation-sensitive hematopoietic elements that could be activated by cytokines released by the CTL. In these animals, the number of splenocytes was reduced to <1% of control levels at the time of CTL injection (data not shown). As illustrated in Fig. 6 *B*, the kinetics of liver disease was delayed ~24 h by prior irradiation, suggesting that radiosensitive inflammatory cells, such as mature lymphocytes and PMN, may contribute to pathogenesis during the first 24 h after CTL injection. Interestingly, the necroinflammatory foci (step 2) that characteristically appear during this time period, and are composed of lymphocytes, monocyte/macrophages, and neutrophils, were greatly diminished in size and number in the irradiated animals, despite the development of apoptotic hepatocytes and broad zones of hypereosinophilic necrotic hepatocytes and the appearance of hyperplastic sinusoidal lining cells by 72 h after CTL administration (Fig. 7 *C*). Importantly, although the total number of splenocytes was greatly reduced by irradiation (see above), the number of splenic and hepatic macrophages, detectable histologically by carbon particle ingestion, was quantitatively and qualitatively normal in irradiated animals (Fig. 8 *A*). These results indicate that step 2 (necroinflammatory foci) of this disease process is mediated by CTL-activated radiosensitive host-derived inflammatory cells, and they suggest that radioresistant cells (e.g., monocyte/macrophages) are responsible for progression to step 3 (widespread hepatic necrosis).

Effects of Carrageenan. Since tissue macrophages are known to be radioresistant and to be activated strongly by IFN-γ (33–36), and since they are a major constituent of the intrahepatic inflammatory cell infiltrate after transfer of CTL (Fig. 5 *D*), we pretreated groups of CTL recipients with carrageenan to inactivate tissue macrophages in order to assess the role they might play in this model. In these studies, carrageenan was injected intraperitoneally daily for 5 d before CTL injection. Carrageenan administered in this manner is known to be toxic for tissue macrophages (26, 27, 36). As illustrated in Fig. 6 *C*, carrageenan treatment reduced the severity of liver disease by >85% at all time points ($p < 0.0005$), suggesting that carrageenan-sensitive cells (presumably macrophages) play an important role in this disease model. As shown in Fig. 8 *B*, the number of carbon particle–positive phagocytic cells in the liver and spleen were either greatly reduced or abolished, respectively, after treatment with carrageenan. Whereas this was associated with a profound reduction in the widespread hepatic necrosis (step 3) normally seen in the context of HBsAg retention in this model, carrageenan treatment had no effect on the development of hepatocellular apoptosis (Fig. 7 *D*, asterisks) or necroinflammatory foci (Fig. 7 *D*, arrowheads), indicating that carrageenan did not inhibit these direct or indirect effects of the CTL. Furthermore, it is important to note that carrageenan alone had no effect on sALT levels in control animals (data not shown).

Collectively, the foregoing observations suggest that step 1 in this disease process is caused by a direct effect of the CTL on the hepatocyte, that step 2 is mediated by radiosensitive, carrageenan-resistant inflammatory cells that are activated by one or more antigen nonspecific CTL products that have not yet been identified, and that step 3 reflects the selective destruction of hepatocytes that retain HBsAg by carrageenan-sensitive, radiation-resistant phagocytic cells that have been activated by IFN-γ secreted by antigen-reactive CTL. The data also suggest that disease evolution to step 3 does not require passage through stage 2.

Discussion

The current study describes the immunopathological characterization of a fatal necroinflammatory liver disease in HBsAg-positive transgenic mice that is initiated by HBsAg-specific, MHC class I (L^d)–restricted, CD8-positive CTL clones that secrete IFN-γ after antigen recognition. Several features of this experimental system created the opportunity to dissect the molecular and cellular mechanisms responsible for class I–restricted immunopathology in vivo, in a disease model that closely resembles HBV-induced fulminant hepatitis.

First, the class I–restricted CTL clones employed in these

Figure 7. Modulation of CTL-induced liver disease by irradiation, anti-IFN-γ, and carrageenan. Histopathological characteristics of liver disease 72 h after CTL administration to otherwise untreated transgenic mice (*A*), mice pretreated with antibodies to IFN-γ (*B*), irradiated with 900 rad (*C*), or injected with carrageenan (*D*). (*A*) Note the mixed inflammatory cell infiltrate throughout the hepatic lobule extending from the portal tract (*PT*) to the central vein (*CV*), and the accompanying broad zones of hepatocellular necrosis, microvesicular steatosis, and ballooning degeneration. Note also the presence of many hyperplastic sinusoidal lining cells widely distributed throughout the section. (*B*) Note the absence of widespread necrosis compared with *A* and *C*, and the marked reduction in inflammatory cells despite the presence of apoptotic hepatocytes (*). Rare, small necroinflammatory foci are observed (*arrowheads*), representing the most severe manifestation of the disease observed in these animals. Note also that the sinusoidal lining cells appear to be less hyperplastic than in *A*, *C*, and *D*. (*C*) Note the marked reduction of inflammatory cells but the presence of many hyperplastic sinusoidal lining cells and a broad zone of necrotic hepatocytes displaying condensed eosinophilic cytoplasm that extends diagonally across the field toward the central vein. Apoptotic hepatocytes are plentiful within the field (*). (*D*) Note the absence of widespread necrosis compared with *A* and *C* despite a fairly abundant, mixed inflammatory cell infiltrate and hyperplastic sinusoidal lining cells, numerous apoptotic hepatocytes (*) and multiple necroinflammatory foci (*arrowheads*). This is the most severe stage in the CTL-induced lesion observed in carrageenan-treated mice. All panels stained with hematoxylin and eosin; original magnification ×200).

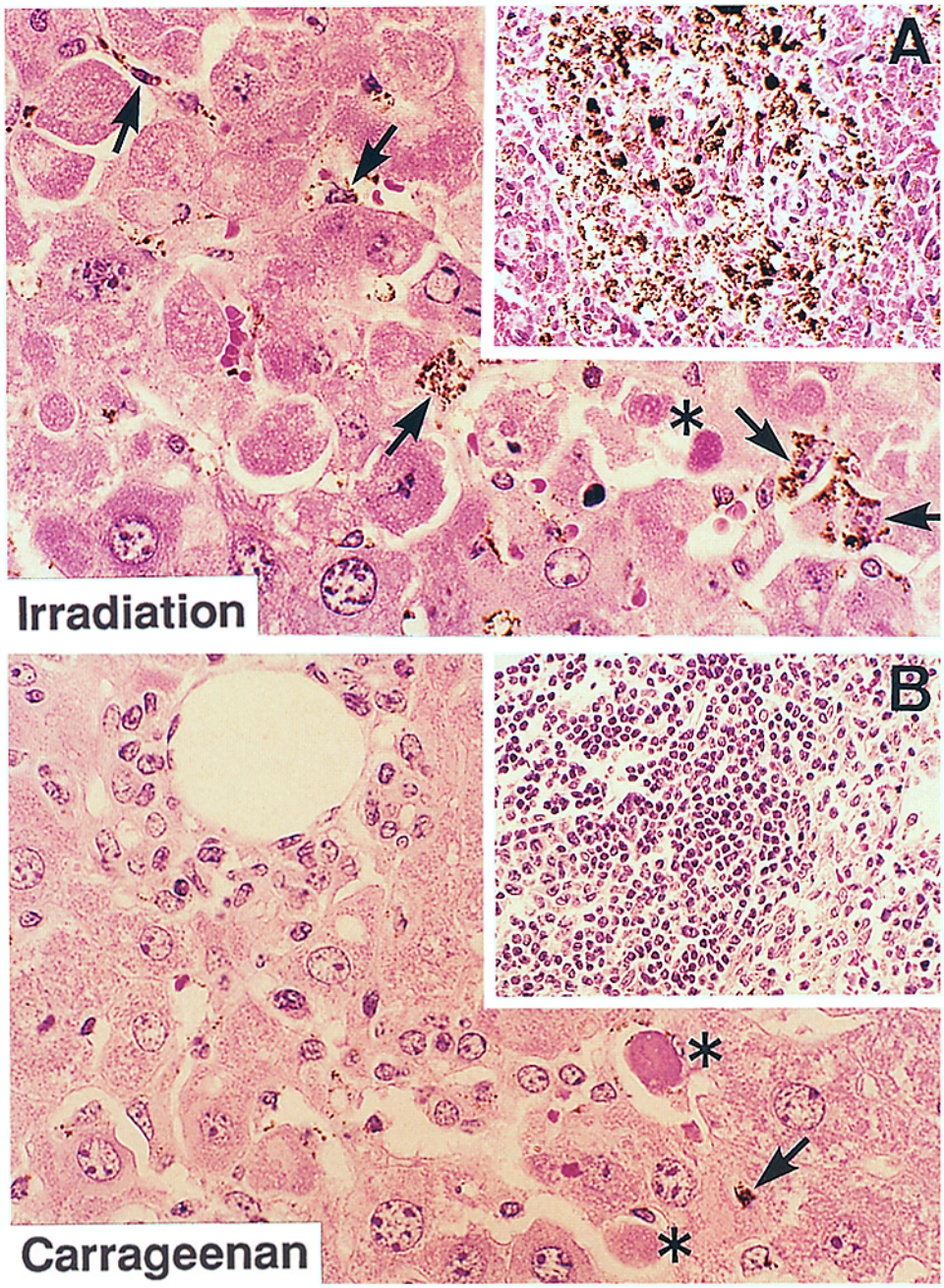

Figure 8. Role of radioresistant, phagocytic cells in disease pathogenesis. Groups of three lineage 107-5D males were either irradiated (900 rad) or injected intraperitoneally with carrageenan 6 d before, or daily for 5 d, respectively, before the injection of 10^7 CTL. Mice were injected intravenously with India ink on day 2 after CTL (to permit assessment of phagocytic cells in situ) and they were killed for histopathological analysis on day 3. (*A*) Note the presence of numerous black pigment (carbon particle)–laden macrophages in the hepatic sinusoids (*arrows*) and in the collapsed marginal zone of the splenic white pulp (*inset*) indicating the radioresistant properties of this cell type, in contrast to the relative paucity of nonphagocytic inflammatory cells in both tissues. Despite depletion of radiosensitive cells, many apoptotic (*) and necrotic hepatocytes are present in the liver. (*B*) In contrast, depletion of phagocytic cells in carrageenan-treated animals, evidenced by a marked reduction in the number of carbon particle–laden macrophages in the liver (*arrow*) and the splenic white pulp (*inset*), liver disease severity is markedly decreased, even though both tissues display abundant numbers of carbon particle negative, i.e., nonphagocytic, inflammatory cells in both tissues.

studies are specific for an epitope (HBsAg25-39) which is conserved in all known HBV isolates. Furthermore, all of the CTL lines and clones that we have established thus far in B10.D2 mice have displayed the same antigenic fine specificity suggesting that this epitope is immunodominant in the context of the H-2^d haplotype. Additionally, it overlaps an HLA-A2–restricted CTL epitope that is recognized by patients with acute viral hepatitis (Chisari, F. V., unpublished observations) and it also overlaps an HLA-DPw4-restricted helper T cell epitope that is recognized by HBsAg vaccine recipients (37, 38). Thus, it would appear that this highly conserved viral sequence is also highly immunogenic for human T cells, and therefore it may be relevant in the pathogenesis of viral hepatitis in humans. Second, HBsAg is expressed in 100% of the hepatocytes in two of the lineages (107-5 and pFC80-219) used in this study (22), so that every hepatocyte is a potential target for cytolytic attack when the CTL are transferred in vivo. Third, the HBsAg-positive hepatocyte is known to be exquisitely sensitive to the hepatocytotoxic effects of IFN-γ (24) which is produced by the CTL clone used in this study, and by all of the HBsAg-specific CTL clones we have derived thus far. Fourth, the unique microanatomy of the hepatic sinusoid, which contains a discontinuous endothelium and lacks a basement membrane (39,

40), simultaneously grants the CTL direct and immediate access to the target hepatocytes, which they have the potential to kill, and to the resident intrahepatic macrophages (Kupffer cells), which they have the potential to activate. Finally, CTL entry and localization within the liver, their ability to bind and kill the HBsAg-positive hepatocyte, and their capacity to activate an intrahepatic inflammatory response can all be experimentally identified and quantitated, thereby making each of these aspects of CTL function individually discernible in vivo in this model.

Taking advantage of these features, we demonstrated that the CTL-induced necroinflammatory liver disease displays stepwise progression from single cell necrosis to massive destruction of most hepatocytes, and it displays most of the immunohistochemical and histopathological characteristics of HBV-induced acute hepatitis in humans. The stepwise nature of the disease process was evident upon quantitative morphometric histopathological analysis of the liver at increasing time points after the injection of BrdU-labeled CTL.

Step 1 begins, within 1 h of CTL administration, with antigen recognition by the CTL and delivery of a signal that results in the death of the hepatocyte by a process that displays all of the cytological criteria of apoptosis. The fact that this process is not inhibited by the prior administration of antibodies to IFN-γ indicates that it is not mediated by this cytokine. This event appears to be pathogenetically limited to very few cells, however, possibly because free-ranging CTL movement is severely limited by the architectural constraints of solid tissue. The direct CTL–target cell interaction results in widely scattered, acidophilic, Councilman bodies (apoptotic hepatocytes) that are characteristic of acute viral hepatitis in humans (31, 32). As we have recently reported in detail (Ando, K. et al., manuscript submitted for publication), this model provides the first definitive demonstration that class I–restricted CTL can directly destroy their target cells in vivo.

Step 2 begins 4–12 h later, when the CTL recruit many BrdU-negative (i.e., host-derived) inflammatory cells into their immediate vicinity, resulting in the formation of necroinflammatory foci and the extension of hepatocellular apoptosis and lysis to the periphery of necroinflammatory foci well beyond the CTL. The histopathological features of step 2 were abrogated by lethal irradiation, which also caused a 24-h delay in the disease process, indicating that radiation-sensitive lymphocytes and neutrophils probably contribute importantly to this aspect of the disease. On the contrary, it would appear that the circulating monocytes and intrahepatic sinusoidal macrophages (Kupffer cells) do not play a major role in step 2, since the number of phagocytically active macrophages in the liver was not affected by irradiation, and since necroinflammatory foci were observed in mice whose intrahepatic macrophages had been functionally inactivated by the prior injection of carrageenan. Although we presume that step 2 is mediated by secretion of one or more cytokines by the antigen-activated CTL, this component of the disease was not completely blocked by anti-IFN-γ antibodies, suggesting either that IFN-γ is not necessary for development of this stage of the disease, or that the antibodies failed to efficiently reach the interior of these necrotic foci. The latter is unlikely in view of the profound effect of anti-IFN-γ on step 3 in the disease process. Because the histopathology of typical acute viral hepatitis in humans (31, 32) is quite similar to the mouse liver at this stage (apoptotic hepatocytes, focal necroinflammatory lymphomononuclear cell infiltrates and Kupffer cell hyperplasia), it is quite possible that the same events that are responsible for steps 1 and 2 in the current disease model may be pathogenetically responsible for the liver disease typical of acute, nonfatal viral hepatitis B in humans.

Step 3 is detectable 24–72 h after CTL administration, when the livers display massive hepatocellular necrosis and an inflammatory cell infiltrate that consists principally of host-derived lymphomononuclear cells and pronounced sinusoidal lining cell (Kupffer cell?) hyperplasia, resembling the histopathological changes observed in patients dying from liver failure due to HBV-induced fulminant hepatitis (31). The inflammatory cells, especially the monocyte/macrophages, outnumber the injected CTL by at least 100-fold at this point in the disease process, suggesting that they might serve to amplify the cytopathic effects of the CTL to the extent of massive hepatocellular necrosis and the death of the mouse. Since the pathogenetic effect of the CTL was reduced more than 97% by the prior administration of neutralizing mAbs to IFN-γ, which also reduced the CTL-induced mortality rate to zero, it would appear that this cytokine is principally responsible for the extreme severity of the liver disease in this model.

IFN-γ is known to activate macrophages (33–35) and to mediate the recruitment of lymphocytes into typical class II–restricted DTH reactions (41). This cytokine is also known to be secreted by many $CD8^+$ murine clones in response to antigenic stimulation (42). Accordingly, it has been shown that CTL-induced clearance of influenza virus in vivo correlates with the ability of the virus-specific CTL clones to secrete IFN-γ and induce a DTH reaction upon exposure to antigen (43). Interestingly, tumor regression mediated by cultured tumor-infiltrating $CD8^+$ lymphocytes correlates better with their ability to secrete IFN-γ than with their cytotoxic potential in vitro (44), and several groups have shown that tumor regression can be induced by a DTH reaction that is mediated by IFN-γ activated macrophages (27, 33, 34, 45, 46). Furthermore, $CD8^+$ T cell protection in rodent models of *Plasmodium berghei* (47) and *Toxoplasma gondii* infection (48) are dependent on IFN-γ, although the control of murine *Listeria monocytogenes* infection by $CD8^+$ T cells appears to be independent of IFN-γ (49). Finally, Doherty et al. (50) have suggested that LCMV-induced murine choriomeningitis may be mediated by a massive DTH reaction that is triggered by relatively few virus-immune CD8-positive T cells but is composed principally of antigen-nonspecific monocytes and macrophages.

In view of the foregoing, and since the severity of liver disease in the current model was also profoundly reduced in mice whose macrophage function had been blocked by multiple injections of carrageenan, we conclude that IFN-γ activated intrahepatic macrophages are probably responsible for the massive, fatal hepatocellular necrosis characteristic of step

3 in this model. Based on previous reports that apoptotic cells can prime macrophages to activation by IFN-γ in vitro (43), it is possible (although not proven) that CTL-induced hepatocellular apoptosis might cooperate with IFN-γ to create the massive lesion we observed in these animals. It is important to emphasize that the extreme severity of this phase of the disease process (step 3) depends on the fact that HBsAg retention sensitizes the hepatocyte to the cytopathic effects of IFN-γ (25) since the disease did not progress beyond step 2 in lineage pFC80-219D whose hepatocytes secrete HBsAg rather than retain it. We conclude, therefore, that the CTL serve as highly efficient IFN-γ delivery vehicles, resulting in widespread activation of intrahepatic macrophages that, in the context of widespread HBsAg retention, eventually destroy most or all of the HBsAg-positive hepatocytes and kill the mice. Additional studies will be necessary to identify the specific macrophage function or product that is responsible for this devastating effect.

Although our data indicate that class I–restricted immunopathology is a stepwise process in this model system, it is likely that the three steps are sequential yet independent responses to differing signals delivered by antigen-activated CTL. In view of the close physical approximation of CTL and hepatocyte and the associated cytological features of apoptosis, it would appear that step 1 represents a direct effect of the CTL in vivo, similar to the ability of CTL to induce apoptosis by direct interaction with target cells in vitro. Apoptosis, however, is usually not a proinflammatory event. Accordingly, we suggest that the focal (step 2) and generalized (step 3) necroinflammatory reactions that occur later in this model are due to independent indirect functions of the CTL that are mediated by IFN-γ and other currently unidentified cytokines.

Based on the similarities between this model and the immunopathological features of human viral hepatitis, with most cases of acute and chronic hepatitis displaying the histological features of steps 1 and 2, while fulminant hepatitis resembles progression to step 3, we suggest that comparable events contribute to the pathogenesis of liver disease during HBV infection in humans. We also suggest that the general principles illustrated in this study may be applicable to other models of class I–restricted immunopathology as well.

The authors thank Dr. Yasutoshi Muto (Gifu University, Gifu, Japan) for encouragement and support. We also thank Drs. J. Langhorne and S. Landolfo for providing 01.E70.3B2 and AN18.03.C12 hybridomas, Dr. Gabriele Missale for helpful discussion, Ms. Debbie Guerrette and Violet Martinez for breeding and maintenance of the transgenic mouse colony, Ms. Margie Pagels for excellent histological services, and Ms. Bonnie Weier for manuscript preparation. Transgenic mouse lineages 107-5 and 23-3 were produced in collaboration with Drs. Ralph Brinster (University of Pennsylvania, Philadelphia, PA) and Richard Palmiter (University of Washington, Seattle, WA). This is manuscript number 7791-MEM from The Scripps Research Institute.

This work was supported by grants R37-CA40489 and CA54560 from the National Cancer Institute, and by a fellowship from Genentech, Inc. K. Ando was supported by funds from the Chiiki Iryo Foundation (Gifu, Japan). S. Wirth was supported in part by a fellowship of the Swiss National Fund for Scientific Research. L. G. Guidotti was supported by a fellowship from the University of Parma (Parma, Italy).

Address correspondence to Dr. Francis V. Chisari, The Scripps Research Institute, Division of Experimental Pathology, 10666 North Torrey Pines Road (SBR-10), La Jolla, CA 92037. K. Ando is currently at the First Department of Internal Medicine, Gifu University Medical School, Gifu, Japan; T. Moriyama is currently at the Department of Gastroenterology, Jichi Medical School, Kawachi-gun, Tochigi, Japan; and S.-N. Huang is currently at the Department of Pathology, Sunnybrook Health Science Centre, University of Toronto, Ontario, Canada.

Received for publication 27 May 1993 and in revised form 12 July 1993.

References

1. Walker, C.M., D.J. Moody, D.P. Stites, and J.A. Levy. 1986. $CD8^+$ Lymphocytes can control HIV infection in vitro by suppressing virus replication. *Science (Wash. DC).* 234:1563.
2. Walker, C.M., A.L. Erickson, F.C. Hsueh, and J.A. Levy. 1991. Inhibition of human immunodeficiency virus replication in acutely infected $CD4^+$ cells by $CD8^+$ cells involves a noncytotoxic mechanism. *J. Virol.* 65:5921.
3. Martz, E., and S.R. Gamble. 1992. How do CTL control virus infections? Evidence for prelytic halt of Herpes simplex. *Viral Immunol.* 5:81.
4. Eichelberger, M., W. Allan, M. Zijlstra, R. Jaenisch, and P.C. Doherty. 1991. Clearance of Influenza virus respiratory infection in mice lacking class I major histocompatibility complex–restricted $CD8^+$ T cells. *J. Exp. Med.* 174:875.
5. Lehmann-Grube, F., U. Assmann, C. Löliger, D. Moskophidis, and J. Löhler. 1985. Mechanism of recovery from acute virus infection. I. Role of T lymphocytes in the clearance of lymphocytic choriomeningitis virus from spleens of mice. *J. Immunol.* 134:608.
6. Kaufman, D.B., J.L. Platt, F.L. Rabe, D.L. Dunn, F.H. Bach,

and D.E.R. Sutherland. 1990. Differential roles of Mac-1$^+$ cells, and CD4$^+$ and CD8$^+$ T lymphocytes in primary nonfunction and classic rejection of islet allografts. *J. Exp. Med.* 172:291.

7. Rosenberg, A.S., T.I. Munitz, T.G. Maniero, and A. Singer. 1991. Cellular basis of skin allograft rejection across a class I major histocompatibility barrier in mice depleted of CD8$^+$ T cells in vivo. *J. Exp. Med.* 173:1463.
8. Alexander, R.B., and S.A. Rosenberg. 1990. Long term survival of adoptively transferred tumor-infiltrating lymphocytes in mice. *J. Immunol.* 145:1615.
9. Falkenburg, J.H.F., H.M. Goselink, D. Van der Harst, S.A.P. Van Luxemburg-Heijs, Y.M.C. Kooy-Winkelaar, L.M. Faber, J. De Kroon, A. Brand, W.E. Fibbe, R. Willemze, and E. Goulmy. 1991. Growth inhibition of clonogenic leukemic precursor cells by minor histocompatibility antigen–specific cytotoxic T lymphocytes. *J. Exp. Med.* 174:27.
10. Anderson, J., J.A. Byrne, R.D. Schreiber, S. Patterson, and M.B.A. Oldstone. 1985. Biology of cloned cytotoxic T lymphocytes specific for lymphocytic choriomeningitis virus: Clearance of virus and in vitro properties. *J. Virol.* 53:552.
11. Zinkernagel, R.M., E. Haenseler, T. Leist, A. Cerny, H. Hengartner, and A. Althage. 1986. T cell–mediated hepatitis in mice infected with lymphocytic choriomeningitis virus. Liver cell destruction by H-2 class I–restricted virus specific cytotoxic T cells as a physiological correlate of the ^{51}Cr-release assay. *J. Exp. Med.* 164:1075.
12. Koh, D.R., W.P. Fung-Leung, A. Ho, D. Gray, H. Acha-Orbea, and T.W. Mak. 1992. Less mortality but more relapse in experimental allergic encephalomyelitis in CD8$^{-/-}$ mice. *Science (Wash. DC).* 256:1210.
13. Jiang, H., S.L. Zhang, and B. Pernis. 1992. Role of CD8$^+$ T cells in murine experimental allergic encephalomyelitis. *Science (Wash. DC).* 256:1213.
14. Lemire, J.M., and W.O. Weigle. 1986. Passive transfer of experimental allergic encephalomyelitis by myelin basic protein-specific L3T4$^+$ T cell clones possessing several functions. *J. Immunol.* 137:3169.
15. Sriram, S., L. Carroll, S. Fortin, S. Cooper, and G. Ranges. 1988. In vivo immunomodulation by monoclonal anti CD4 antibody. II. Effect on T cell response to myelin basic protein and experimental allergic encephalomyelitis. *J. Immunol.* 141:464.
16. Acha-Orbea, H., D.J. Mitchell, L. Timmermann, D.C. Wraith, G.S. Tausch, M.K. Waldor, S.S. Zamvil, H.O. McDevitt, and L. Steinman. 1988. Limited heterogeneity of T cell receptors from lymphocytes mediating autoimmune encephalomyelitis allows specific immune intervention. *Cell.* 54:263.
17. Romball, C.G., and W.O. Weigle. 1987. Transfer of experimental autoimmune thyroiditis with T cell clones. *J. Immunol.* 138:1092.
18. Tung, K.S.K., T.D. Yule, C.A. Mahi-Brown, and M.B. Listrom. 1987. Distribution of histopathology and Ia positive cells in actively induced and passively transferred experimental autoimmune orchitis. *J. Immunol.* 138:752.
19. Bendelac, A., C. Carnaud, C. Boitard, and J.F. Bach. 1987. Syngeneic transfer of auto-immune diabetes from diabetic NOD mice to healthy neonates. Requirement for both L3T4$^+$ and Lyt-2$^+$ T cells. *J. Exp. Med.* 166:823.
20. Moriyama, T., S. Guilhot, K. Klopchin, B. Moss, C.A. Pinkert, R.D. Palmiter, R.L. Brinster, O. Kanagawa, and F.V. Chisari. 1990. Immunobiology and pathogenesis of hepatocellular injury in hepatitis B virus transgenic mice. *Science (Wash. DC).* 248:361.
21. Chisari, F.V., P. Filippi, A. McLachlan, D.R. Milich, M. Riggs, S. Lee, R.D. Palmiter, C.A. Pinkert, and R.L. Brinster. 1986. Expression of hepatitis B virus large envelope polypeptide inhibits hepatitis B surface antigen secretion in transgenic mice. *J. Virol.* 60:880.
22. Chisari, F.V., P. Filippi, J. Buras, A. MacLachlan, H. Popper, C.A. Pinkert, R.D. Palmiter, and R.L. Brinster. 1987. Structural and pathological effects of synthesis of hepatitis B virus large envelope polypeptide in transgenic mice. *Proc. Natl. Acad. Sci. USA.* 84:6909.
23. Gilles, P.N., G. Fey, and F.V. Chisari. 1992. Tumor necrosis factor alpha negatively regulates hepatitis B virus gene expression in transgenic mice. *J. Virol.* 66:3955.
24. Gilles, P.N., D.L. Guerrette, R.J. Ulevitch, R.D. Schreiber, and F.V. Chisari. 1992. HBsAg retention sensitizes the hepatocyte to injury by physiological concentrations of interferon-γ. *Hepatology.* 16:655.
25. Chisari, F.V., K. Klopchin, T. Moriyama, C. Pasquinelli, H.A. Dunsford, S. Sell, C.A. Pinkert, R.L. Brinster, and R.D. Palmiter. 1989. Molecular Pathogenesis of hepatocellular carcinoma in hepatitis B virus transgenic mice. *Cell.* 59:1145.
26. Shu, S., L.S. Fonseca, H. Kato, and B. Zbar. 1983. Mechanisms of immunological eradication of a syngeneic guinea pig tumor: participation of a component(s) of recipient origin in the expression of systemic adoptive immunity. *Cancer Res.* 43:2637.
27. Mulé, J.J., M. Rosenstein, S. Shu, and S.A. Rosenberg. 1985. Eradication of a disseminated syngeneic mouse lymphoma by systemic adoptive transfer of immune lymphocytes and its dependence upon a host component(s). *Cancer Res.* 45:526.
28. Van Rooijen, N., and R. Van Nieuwmegen. 1984. Elimination of phagocytic cells in the spleen after intravenous injection of liposome-encapsulated dichloromethylene diphosphonate. An enzyme-histochemical study. *Cell Tissue Res.* 238:355.
29. Sheehan, K.C.F., N.H. Ruddle, and R.D. Schreiber. 1989. Generation and characterization of hamster monoclonal antibodies that neutralize murine tumor necrosis factors. *J. Immunol.* 142:3884.
30. Schreiber, R.D., L.J. Hicks, A. Celada, N.A. Buchmeier, and P.W. Gray. 1985. Monoclonal antibodies to murine γ-interferon which differentially modulate macrophage activation and antiviral activity. *J. Immunol.* 134:1609.
31. Ishak, K.G. 1976. Light microscopic morphology of viral hepatitis. *Am. J. Clin. Pathol.* 65:787.
32. Dienes, H.P., H. Popper, W. Arnold, and H. Lobeck. 1982. Histologic observations in human hepatitis non-A, non-B. *Hepatology.* 2:562.
33. Pace, J.L., S.W. Russell, R.D. Schreiber, A. Altman, and D.H. Katz. 1983. Macrophage activation: priming activity from a T-cell hybridoma is attributable to interferon-γ. *Proc. Natl. Acad. Sci. USA.* 80:3782.
34. Pace, J.L., S.W. Russell, B.A. Torres, H.M. Johnson, and P.W. Gray. 1983. Recombinant mouse γ-interferon induces the priming step in macrophage activation for tumor cell killing. *J. Immunol.* 130:2011.
35. Buchmeier, N.A., and R.D. Schreiber. 1985. Requirement of endogenous interferon-γ production for resolution of *Listeria monocytogenes* infection. *Proc. Natl. Acad. Sci. USA.* 82:7404.
36. Thomson, A.W., and E.F. Fowler. 1981. Carrageenan: a review of its effects on the immune system. *Agents Actions.* 11:265–273.
37. Celis, E., D. Ou, and L. Otvos, Jr. 1988. Recognition of hep-

atitis B surface antigen by human T lymphocytes. Proliferative and cytotoxic responses to a major antigenic determinant defined by synthetic peptides. *J. Immunol.* 140:1808.
38. Penna, A., P. Fowler, A. Bertoletti, S. Guilhot, B. Moss, R.F. Margolskee, A. Cavalli, A. Valli, F. Fiaccadori, F.V. Chisari, and C. Ferrari. 1992. Hepatitis B virus (HBV)–specific cytotoxic T-cell (CTL) response in humans: characterization of HLA class II–restricted CTLs that recognize endogenously synthesized HBV envelope antigens. *J. Virol.* 66:1193.
39. Rappaport, A.M. 1973. The microcirculatory hepatic unit. *Microvasc. Res.* 6:212.
40. Grisham, J.W., W. Nopanitaya, J. Compagno, and A.E.H. Nägel. 1975. Scanning electron microscopy of normal rat liver: the surface of its cells and tissue components. *Am. J. Anat.* 144:295.
41. Issekutz, T.B., J.M. Stoltz, and P.V.D. Meide. 1988. Lymphocyte recruitment in delayed-type hypersensitivity. The role of IFN-γ. *J. Immunol.* 140:2989.
42. Yamasaki, T., H. Handa, J. Yamashita, Y. Watanabe, Y. Namba, and M. Hanaoka. 1984. Specific adoptive immunotherapy with tumor-specific cytotoxic T-lymphocyte clone for murine malignant gliomas. *Cancer Res.* 44:1776.
43. Lin, Y.L., and B.A. Askonas. 1981. Biological properties of an influenza A virus–specific killer T cell clone. Inhibition of virus replication in vivo and induction of delayed-type hypersensitivity reactions. *J. Exp. Med.* 154:225.
44. Barth, R.J., Jr., J.J. Mulé, P.J. Spiess, and S.A. Rosenberg. 1991. Interferon-γ and tumor necrosis factor have a role in tumor regression mediated by murine $CD8^+$ tumor-infiltrating lymphocytes. *J. Exp. Med.* 173:647.
45. Meltzer, M.S. 1981. Macrophage activation for tumor cytotoxicity: characterization of priming and trigger signals during lymphokine activation. *J. Immunol.* 127:179.
46. Schultz, R.M., and W.J. Kleinschmidt. 1983. Functional identity between murine γ interferon and macrophage activating factor. *Nature (Lond.).* 305:239.
47. Schofield, L., J. Villaquiran, A. Ferreira, H. Schellekens, R. Nussenzweig, and V. Nussenzweig. 1987. γ-interferon, $CD8^+$ T cells and antibodies required for immunity to malaria sporozoites. *Nature (Lond.).* 330:664.
48. Suzuki, Y., and J.S. Remington. 1990. The effect of anti-IFN-γ antibody on the protective effect of Lyt-2^+ immune T cells against toxoplasmosis in mice. *J. Immunol.* 144:1954.
49. Harty, J.T., R.D. Schreiber, and M.J. Bevan. 1992. CD8 T cell can protect against an intracellular bacterium in an interferon γ–independent fashion. *Proc. Natl. Acad. Sci. USA.* 89:11612.
50. Doherty, P.C., J.E. Allan, F. Lynch, and R. Ceredig. 1990. Dissection of an inflammatory process induced by $CD8^+$ T cells. *Immunol. Today.* 11:55.